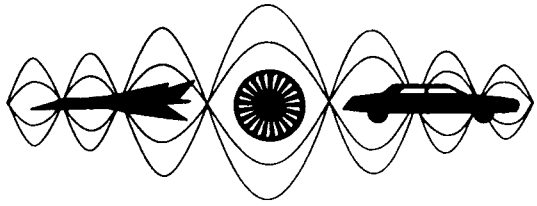

FIFTH INTERNATIONAL CONGRESS ON SOUND AND VIBRATION
DECEMBER 15-18, 1997
ADELAIDE, SOUTH AUSTRALIA

NONSTATIONARY VIBRATIONS IN A CATENARY-VERTICAL HOISTING CABLE SYSTEM

S. Kaczmarczyk
Department of Mechanical Engineering
University of Natal, Durban 4041, South Africa

Abstract

Longitudinal and lateral oscillations in a catenary-vertical hoisting cable system are investigated. The main sources of external excitation in the system are taken into consideration, namely a load due to the winding cycle acceleration/deceleration profile, and a periodic excitation due to the coiling mechanism applied at the winder drum surface. Due to the time-varying length of the vertical cable the natural frequencies and mode shapes of the system vary slowly with time. The system is therefore nonstationary, and its response is qualitatively different from the response of the corresponding stationary parameter system. A mathematical model describing the lateral response of the catenary, and the coupled longitudinal response of the vertical rope, is derived. The non-linear partial-differential equations of motion are discretised by writing the deflections in terms of the linear, free-vibration modes. A non-linear set of ordinary-differential equations with slowly varying coefficients results. The dynamic response of a model example is simulated numerically. The simulation predicts strong modal interactions during a passage through the primary and internal resonances of the system.

1. INTRODUCTION. Hoisting cables, used to carry payloads in inclined and vertical transport systems, are susceptible to vibration which induce dynamic stresses and reduce the useful life of the cables. A common arrangement in industrial hoisting systems comprises a driving winder drum, a steel wire cable, a sheave mounted in headgear, vertical shaft, and a conveyance. The cable passes from the drum over the sheave, forming the horizontal or inclined catenary, to the conveyance in the shaft, forming the vertical rope hanging below the headsheave. Major types of vibration occurring in the hoisting cable systems are classified as longitudinal and lateral vibrations. These vibrations are caused by various sources of excitation. The longitudinal transient response is caused by the winding cycle acceleration/deceleration profile. The primary source of stationary periodic excitation during the constant velocity winding phase, for

both the longitudinal and the lateral response, is formed by a mechanism applied on the winder drum surface in order to achieve a uniform coiling pattern of the cable. The longitudinal vibrations are usually dominant in the vertical rope response, while the lateral vibrations affect mainly the catenary cable. These vibrations excite one another, as a nonlinear coupling exists in the system. Furthermore, the system parameters are changing during the winding cycle due to the time-varying length of the vertical rope, and the natural frequencies and vibration mode shapes vary with time.

The dynamics of hoisting cable systems attracted considerable attention. Investigations into the dynamic response of these systems include the studies reported in references [1]- [5]. In the present paper the coupled lateral-longitudinal oscillations in the hoisting cable system are studied. The classical moving frame approach is used to develop the nonlinear mathematical model representing oscillations in a slowly varying domain. The dynamic response of a model mine hoist system is analyzed through a numerical simulation. A passage through the primary resonances of the system which occur during the winding cycle are evident in the simulated response, and strong modal interactions exist in the system. It is shown that the conditions for the internal resonance arise during the up-wind, promoting further energy exchanges among the modes.

2. EQUATIONS OF MOTION. A model of the hoisting cable system is represented in FIG.1. In this model, the cable is divided into a horizontal catenary of length $OC = L_c$ passing over a sheave of radius R, and of mass moment of inertia I, and into a vertical rope with a mass M, representing the cable payload, attached to its bottom end. The end O_1 of the cable is moving with a prescribed winding velocity $V(t)$ due to the cable being coiled onto a rotating cylindrical drum, so that the entire system translates axially, with the mass M being constrained in a lateral direction. The section $l = OO_1$ represents a slowly varying length of this part of the cable that is already coiled onto the winder drum. The cable has a constant effective cross-sectional area A, a constant mass per unit length m, and effective Young's modulus E.

In order to describe the oscillations of the cable the classical moving frame approach is applied, with the catenary treated as a nonlinear taut string, assuming that there is no cable slip on the drum or across the sheave. Two frames of reference are established: a coordinate system $O_1\bar{x}\bar{y}\bar{z}$ attached to and moving with the upper end of the cable, and a stationary inertial system $OXYZ$. The dynamic deformed position P of an arbitrary section of the cable during its motion is defined in the inertial frame by the position vector

$$\mathbf{R}(s,t) = \mathbf{R}_{O_1}(t) + \bar{\mathbf{R}}^i(s) + \bar{\mathbf{U}}(s,t), \tag{1}$$

where s denotes Lagrangian (material) coordinate of P^i, representing the undeformed position of the cable section, and measured from the origin O_1. In this representation the axial transport motion is treated as essentially an overall rigid body translation, and the dynamic elastic deformations are referred to the moving frame associated with this motion. $\mathbf{R}_{O_1} = [-l, 0, 0]^T$ represents the position of the origin O_1 in the inertial frame, $\bar{\mathbf{R}}^i = [s, 0, 0]^T$ defines the position of P^i, $\bar{\mathbf{U}} = [u(s,t), v(s,t), w(s,t)]^T$ is the dynamic displacement vector from the reference configuration, with u, v, and w representing the

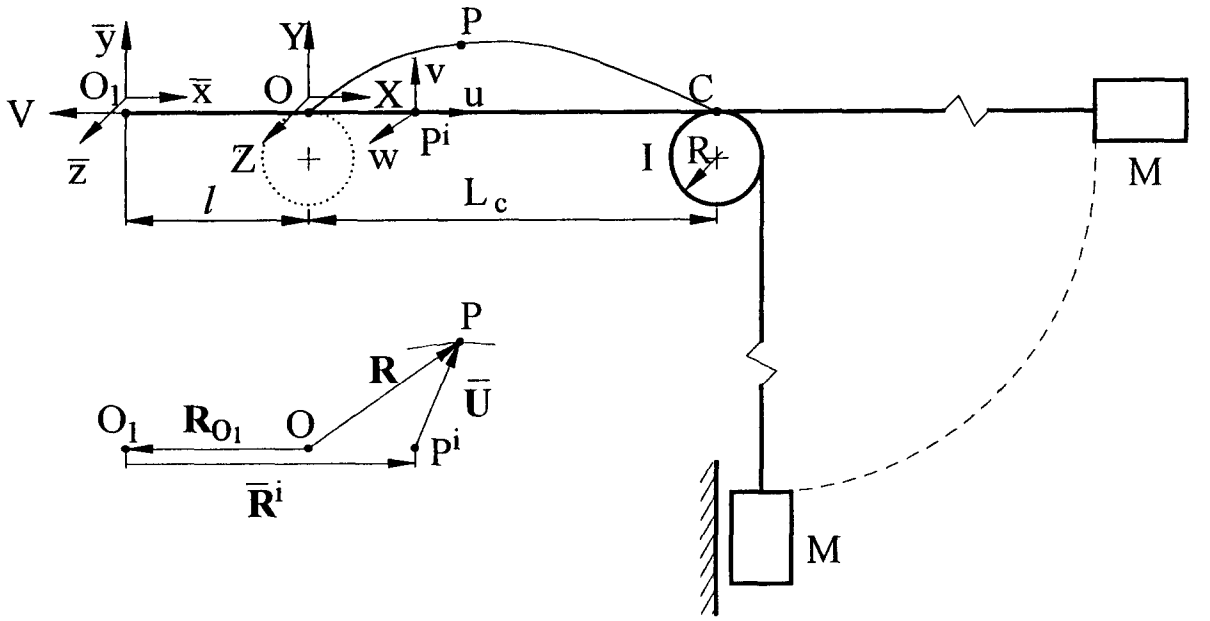

FIG. 1. *Model of the hoisting cable system*

longitudinal, in-plane lateral, and out-of-plane lateral motion, respectively. The upper bar denotes vectors referred to the moving frame. Assuming that there is no lateral motion in the vertical rope, and denoting the longitudinal dynamic deflection in the catenary and in the vertical rope as $u_c(s,t)$ and $u_v(s,t)$, respectively, the deformed position vector is defined as

$$\mathbf{R} = \left\{ \begin{array}{l} [s + u_c(s,t) - l, v(s,t), w(s,t)]^T, \; l \le s \le L_1, \\ [s + u_v(s,t) - l, 0, 0)]^T, \; L_1 \le s \le L_0, \end{array} \right\} \tag{2}$$

where $L_1 = l + L_c$, and L_0 denotes the total length of the cable in the reference configuration. The continuity of deflection across the sheave requires $u_c(L_1,t) = u_v(L_1,t) = u_1$, and the dynamic elastic deflection at the vertical cable bottom end is $u_2 = u_v(L_0,t)$.

The equations of motion of the system can be derived by adopting the methodology used by Perkins and Mote [7] in their study of the nonlinear dynamics of travelling elastic cables. Following this approach, the motion of the hoisting cable is defined by Hamilton's principle

$$\int_{t_1}^{t_2} (\delta E - \delta \Pi_e - \delta \Pi_g)\, dt = 0, \tag{3}$$

where E, Π_e, and Π_g denote the system kinetic energy, the cable elastic strain energy, and the system gravitational potential energy, respectively. Representing the strain measure in the catenary as $\epsilon_c = u_{c,s} + \frac{1}{2}(v_{,s}^2 + w_{,s}^2)$, and in the vertical rope as $\epsilon_v = u_{v,s}$, applying the Hamilton's principle, neglecting the catenary longitudinal inertia, accounting for the boundary excitation due to the winder drum coiling mechanism, defined as $u_c(l,t) = u_l(t)$, $v(l,t) = v_l(t)$, $w(l,t) = w_l(t)$, where u_l, v_l, w_l are periodic,

and applying the coordinate transformation

$$(4) \qquad v(s,t) = \bar{v}(s,t) + v_l(1 - \frac{s-l}{L_c}),\ w(s,t) = \bar{w}(s,t) + w_l(1 - \frac{s-l}{L_c}),$$

and also adding distributed damping forces, the catenary lateral motion is described by the equations

$$(5) \qquad m\bar{v}_{,tt} - T_c^n\bar{v}_{,ss} = EAe(t)\bar{v}_{,ss}) - m\left[\ddot{v}_l(1 - \frac{s-l}{L_c}) + 2\dot{v}_l\frac{\dot{l}}{L_c} + v_l\frac{\ddot{l}}{L_c},\right] + F_{cv},$$

$$(6) \qquad m\bar{w}_{,tt} - T_c^i\bar{w}_{,ss} = EAe(t)\bar{w}_{,ss} - m\left[\ddot{w}_l(1 - \frac{s-l}{L_c}) + 2\dot{w}_l\frac{\dot{l}}{L_c} + w_l\frac{\ddot{l}}{L_c}\right] + F_{cw},$$

defined over the spatial interval $l < s < L_1$, with trivial boundary conditions for $\bar{v}$ and $\bar{w}$ at $s = l, L_1$. In these equations $(\ )_{,s}$ denotes partial differentiation with respect to s, the overdot indicates total differentiation with respect to time, and $(\ )_{,t}$ denotes partial derivatives with respect to time, $T_c^i = [M + m(L_0 - L_1)]g$ represents the slowly varying mean catenary tension, F_{cv} and F_{sw} denote the damping forces, and e represents spatially uniform catenary strain defined as

$$(7) \qquad \begin{aligned} e(t) \ = \ & \frac{1}{L_c}[u_v(L_1,t) - u_l] + \frac{1}{2L_c}\int_l^{L_1}(\bar{v}_{,s}^2 + \bar{w}_{,s}^2)ds + \frac{1}{L_c^2}[\frac{1}{2}(v_l^2 + w_l^2) \\ & - \int_l^{L_1}(v_l\bar{v}_{,s} + w_l\bar{w}_{,s})ds]. \end{aligned}$$

Furthermore, treating the sheave and the payload as additional inertial loads, and adding a damping force represented by F_{cu}, the vertical rope is modeled as the following unrestrained system

$$(8) \qquad \rho u_{v,tt} - EAu_{v,ss} = \rho\ddot{l} - [M_S u_{v,st}\dot{l} + EAe(t)]\delta(s - L_1) + F_{cu},$$

defined over the spatial interval $L_1 < s < L_0$, with the homogeneous boundary conditions $EAu_{v,s}\ |_{s=L_1,L_0} = 0$. In this equation $M_S = \frac{I}{R^2}$ denotes the effective mass of the sheave, and the mass distribution function is defined as $\rho(s) = m + M_S\delta(s - L_1) + M\delta(s - L_0)$.

An equivalent viscous proportional damping is introduced to represent the overall damping effort in the hoisting cable. In this damping model a distributed damping force is expressed in terms of a operator which is a linear combination of the stiffness operator and the mass distribution function. Hence, the lateral damping forces are given as $F_{cv} = -\mathcal{C}[\bar{v}_{,t}]$ and $F_{cw} = -\mathcal{C}[\bar{w}_{,t}]$, respectively, with the damping operator defined as $\mathcal{C} = -\alpha_1 T_c^i\frac{\partial^2}{\partial s^2} + \alpha_2 m$, where α_1 and α_2 are constant coefficients of damping. Similarly, the longitudinal damping force is expressed as $F_{cu} = -\mathcal{C}_u[u_{v,t}]$, with the damping operator given as $\mathcal{C}_u = -\mu_1 EA\frac{\partial^2}{\partial s^2} + \mu_2\rho$, where μ_1 and μ_2 are coefficients of longitudinal damping.

3. DISCRETE MODEL. The equations of motion (5)-(8) are discretised by applying the Rayleigh-Ritz procedure. The dynamic response of the system is approximated by the expansions $\bar{v} = \sum_{n=1}^{N_{lat}} \Phi_n(s,l)p_n(t)$, $\bar{w} = \sum_{n=1}^{N_{lat}} \Phi_n(s,l)q_n(t)$, and $u_v = \sum_{n=1}^{N_{long}} Y_n(s,l)z_n(t)$, where p_n, q_n, and z_n are generalized coordinates, and Φ_n, and Y_n are linear free-oscillation modes of the corresponding undamped stationary system. The in-plane and the out-of-plane modes Φ_n, are equivalent to those of a taut string, so that $\Phi_n = \sin[\frac{n\pi}{L_c}(s-l)]$. The corresponding natural frequencies are given as $\bar{\omega}_n(l) = \frac{n\pi}{L_c}\bar{c}$, where $\bar{c} = \sqrt{T_c^i(l)/m}$. The shape functions Y_n are normal longitudinal modes of the corresponding linear unrestrained system with l being fixed, and are given as $Y_n(s,l) = \cos\gamma_n y(s,l) - \frac{M_s}{m}\gamma_n \sin\gamma_n y(s,l)$, where $\gamma_n = \frac{\omega_n(l)}{c}$, with $c = \sqrt{EA/m}$, ω_n representing the longitudinal natural frequency, and $y = s - l - L_c$. The eigenvalues γ_n are determined from the frequency equation

$$(9) \qquad \frac{M_s}{m}\gamma_n^2(\cos\gamma_n L_v - \frac{M}{m}\gamma_n \sin\gamma_n L_v) + \gamma_n(\frac{M}{m}\gamma_n \cos\gamma_n L_v + \sin\gamma_n L_v) = 0,$$

where $L_v = L_0 - l - L_c$.

In this formulation, the catenary strain (7) is expressed as $e(t) = F_e(t) + \frac{1}{L_c}\sum_{n=1}^{N_{long}} z_n + \sum_{n=1}^{N_{lat}} \beta_n^2(p_n^2 + q_n^2)$, where $F_e(t) = \frac{1}{L_c}\left\{\frac{1}{2L_c}[v_l^2(t) + w_l^2(t)] - u_l(t)\right\}$, and $\beta_n = \frac{n\pi}{2L_c}$, and the discretised lateral equations are

$$\begin{aligned}\ddot{p}_r + 2\bar{\zeta}_r\bar{\omega}_r\dot{p}_r + \bar{\omega}_r^2\left[1 + \left(\frac{c}{\bar{c}}\right)^2 F_e(t)\right]p_r &= -\frac{2}{m_r}\dot{l}\sum_{n=1}^{N_{lat}} C_{rn}\dot{p}_n - \frac{1}{m_r}\sum_{n=1}^{N_{lat}}\left(\dot{l}^2 D_{rn} + \ddot{l}C_{rn}\right)p_n \\ &- \left(\frac{c}{\bar{c}}\right)^2 \bar{\omega}_r^2\left[\frac{1}{L_c}\sum_{n=1}^{N_{long}} z_n + \sum_{n=1}^{N_{lat}}\beta_n^2(p_n^2 + q_n^2)\right]p_r + P_r(t),\end{aligned}$$

(10)

$$\begin{aligned}\ddot{q}_r + 2\zeta_r\bar{\omega}_r\dot{q}_r + \bar{\omega}_r^2\left[1 + \left(\frac{c}{\bar{c}}\right)^2 F_e(t)\right]q_r &= -\frac{2}{m_r}\dot{l}\sum_{n=1}^{N_{lat}} C_{rn}\dot{q}_n - \frac{1}{m_r}\sum_{n=1}^{N_{lat}}\left(\dot{l}^2 D_{rn} + \ddot{l}C_{rn}\right)q_n \\ &- \left(\frac{c}{\bar{c}}\right)^2 \bar{\omega}_r^2\left[\frac{1}{L_c}\sum_{n=1}^{N_{long}} z_n + \sum_{n=1}^{N_{lat}}\beta_n^2(p_n^2 + q_n^2)\right]q_r + Q_r(t),\end{aligned}$$

(11)

where $2\bar{\zeta}_r\bar{\omega}_r = \alpha_1\bar{\omega}_r^2 + \alpha_2$, $m_r = m\int_l^{L_1}\Phi_r^2 ds$, $C_{rn} = m\int_l^{L_1}\Phi_r\frac{\partial\Phi_n}{\partial l}ds$, $D_{rn} = m\int_l^{L_1}\Phi_r\frac{\partial^2\Phi_n}{\partial l^2}ds$, $P_r = \frac{1}{m_r}\int_l^{L_1}\Phi_r F_v(s,t)ds$, and $Q_r = \frac{1}{m_r}\int_l^{L_1}\Phi_r F_w(s,t)ds$.

Also, the following longitudinal equation results

$$\begin{aligned}\ddot{z}_r + \mu_2\dot{z}_r + \bar{\omega}_r^2 z_r &= -\frac{1}{m_r^v}\sum_{n=1}^{N_{long}}\left(2\dot{l}C_{rn}^v - EA\Lambda_{rn} - \frac{M_s^2}{m}\dot{l}\gamma_n^2\right)\dot{z}_n \\ &-\frac{1}{m_r^v}\sum_{n=1}^{N_{long}}\left(\dot{l}^2 D_{rn}^v + \ddot{l}C_{rn}^v - EA\dot{l}B_{rn}^v + M_s\dot{l}^2\Gamma_n + \frac{EA}{L_c}\right)z_n \\ &-\frac{EA}{m_r^v}\left[\sum_{n=1}^{N_{lat}}\beta_n^2(p_n^2 + q_n^2) + F_e(t)\right] + Z_r(t),\end{aligned} \qquad (12)$$

where $m_r^v = \int_{L_1}^{L_0}\rho(s)Y_r^2 ds$, $B_{rn}^v = \int_{L_1}^{L_0}\mu_1(s)Y_r\frac{\partial Y_n''}{\partial l}ds$, $C_{rn}^v = \int_{L_1}^{L_0}\rho(s)Y_r\frac{\partial Y_n}{\partial l}ds$, $D_{rn}^v = \int_{L_1}^{L_0}\rho(s)Y_r\frac{\partial^2 Y_n}{\partial l^2}ds$, $\Gamma_n = \gamma_n(\gamma_n - 2\frac{M_s}{m}\frac{d\gamma_n}{dl})$, $\Lambda_{rn} = \int_{L_1}^{L_0}\mu_1(s)Y_r Y_n''ds$, and $Z_r(t) = \frac{1}{m_r^v}\ddot{l}\int_{L_1}^{L_0}\rho(s)Y_r ds$, with primes denoting partial derivatives with respect to s.

Due to the nonlinear and nonstationary nature of the system, a complex dynamic behaviour of the system can be expected during the winding cycle, when certain frequency tuning conditions are achieved. This is demonstrated in the model example below.

4. NUMERICAL EXAMPLE AND RESULTS. The equations (10)- (12) do not easily lend themselves to analytical solution, and the dynamic response of the system is analyzed through a direct numerical integration. The following parameters, being an example of a mine hoist system arrangement, are assumed in the numerical simulation: $M = 17584\ kg$, $I = 15200\ kg$, $m = 8.4\ kg/m$, $L_c = 74.95\ m$, $L_0 = 2174.95\ m$, $A = 0.001028\ m^2$, $E = 1.1 \times 10^{11}\ N/m^2$, $R = 2.13\ m$. The response of this system is investigated during the ascending cycle from the depth of 1500 m. The discrete model nonlinear equations are solved using the MATLAB ode15s variable-order stiff solver, applied with the default numerical differentiation formulas (NDFs), and with the relative accuracy and absolute error tolerances both set to the value of 10^{-6}. The boundary excitation functions are assumed as $u_l(t) = u_0 \cos \Omega t$, $v_l(t) = v_0 \cos \Omega t$, and $w_l(t) = w_0 \cos \Omega t$, respectively. As the cable cross-over occurs twice per drum revolution, the frequency of the excitation is $\Omega = 2\frac{V}{R_d}$. The excitation amplitudes, determined from the geometry of the cross-over zone, are given as $u_0 = R_d\beta\left[\sqrt{1 + \left(\frac{d}{2R_d\beta}\right)^2} - 1\right]$, $v_0 = (1 - \frac{\sqrt{3}}{2})d$, and $w_l = \frac{d}{2}$, respectively, where $d = 0.048\ m$ is the cable diameter, $R_d = 2.14\ m$ is the drum radius, and $\beta = 0.2\ rad$ is the cross-over diametrical arc. The lateral modal damping ratios are assumed as $\bar{\varsigma}_r = 0.05\%$, which is of the order of damping determined by experimental tests carried out by Mankowski [6]. The longitudinal damping coefficient μ_1 is assumed to be a function of the vertical rope mean tension defined as $T_v^i = [M + m(L_0 - s)]g$, $L_1 \leq s \leq L_0$. Following the experimental data reported by Savin and Goroshko [1], this coefficient is determined as $\mu_1 = 10^{-4}(0.5 + \frac{23000}{3500 + 0.75 \times 10^{-5} T_v^i / A})$. The value of the second longitudinal damping coefficient is assumed to be $\mu_2 = 0.159$, as established by tests performed by Constancon [4].

The simulation results, obtained for a cycle with the acceleration/deceleration of $0.77\ m/s^2$ applied over the period of 20 s, are presented in FIG.2 and 3, where the lateral response at $s = l + L_c/4$, the longitudinal response at the sheave and at the conveyance, as well as the cable tensions are plotted vs. the shaft depth. The respective nominal winding velocity is $V = 15.4\ m/s$, which results in the cross-over frequency $\Omega = 14.39\ rad/s$. This produces a complex resonance situation at the depth of approximately 750 m. In this region the excitation frequency is tuned closely to the second lateral ($\Omega \approx \bar{\omega}_2$) as well as to the second longitudinal ($\Omega \approx \omega_2$) natural frequency, with the latter being near twice that of the first lateral natural frequency ($\omega_2 \approx 2\bar{\omega}_1$), promoting autoparametric interactions between the modes. The dynamic response plots reflect the resulting resonance oscillations. Significant in- and out-of-plane lateral motions occur, and a strong nonlinear interaction between the lateral and longitudinal modes can be noticed. This results in large tension oscillations. The tension ratio across the sheave reaches the value of 2, and on the other hand drops to the value of 0.5, at the depth of approximately 500 m, which may result in a frictional slip across the sheave.

5. CONCLUSION. The hoisting cable system comprising a catenary and a vertical rope forms a complex nonstationary oscillatory system. This is evident in the

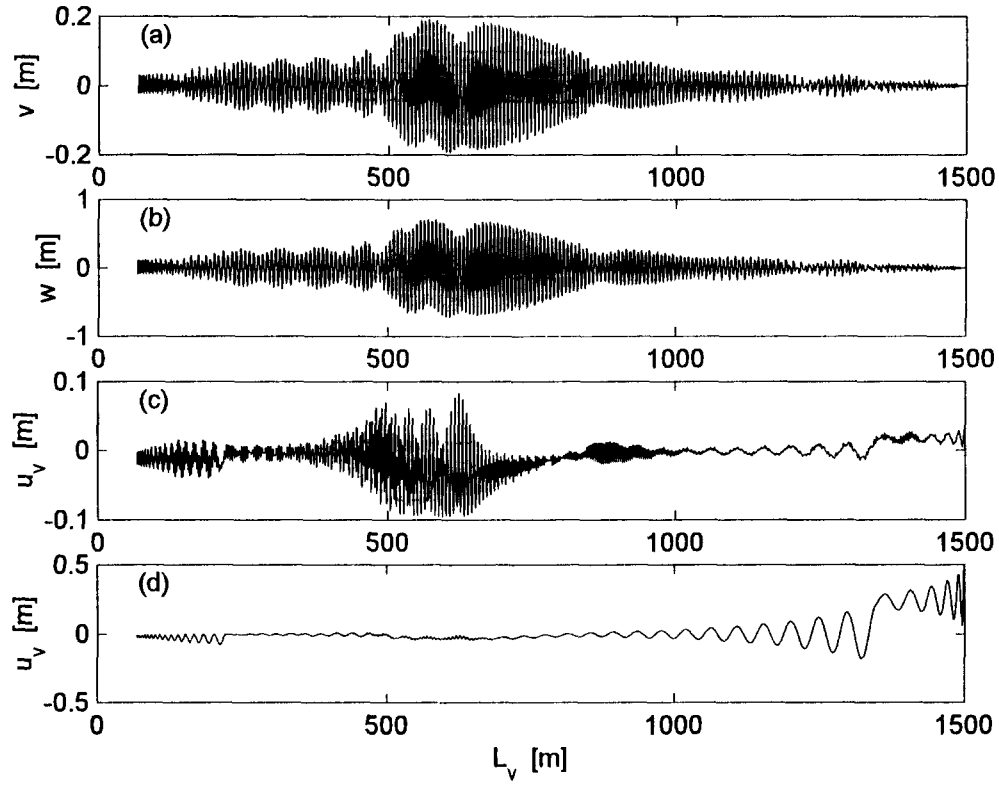

FIG. 2. *Cable response: (a) lateral in-plane, (b) lateral out-of-plane, (c) longitudinal at sheavehead, (d) longitudinal at conveyance.*

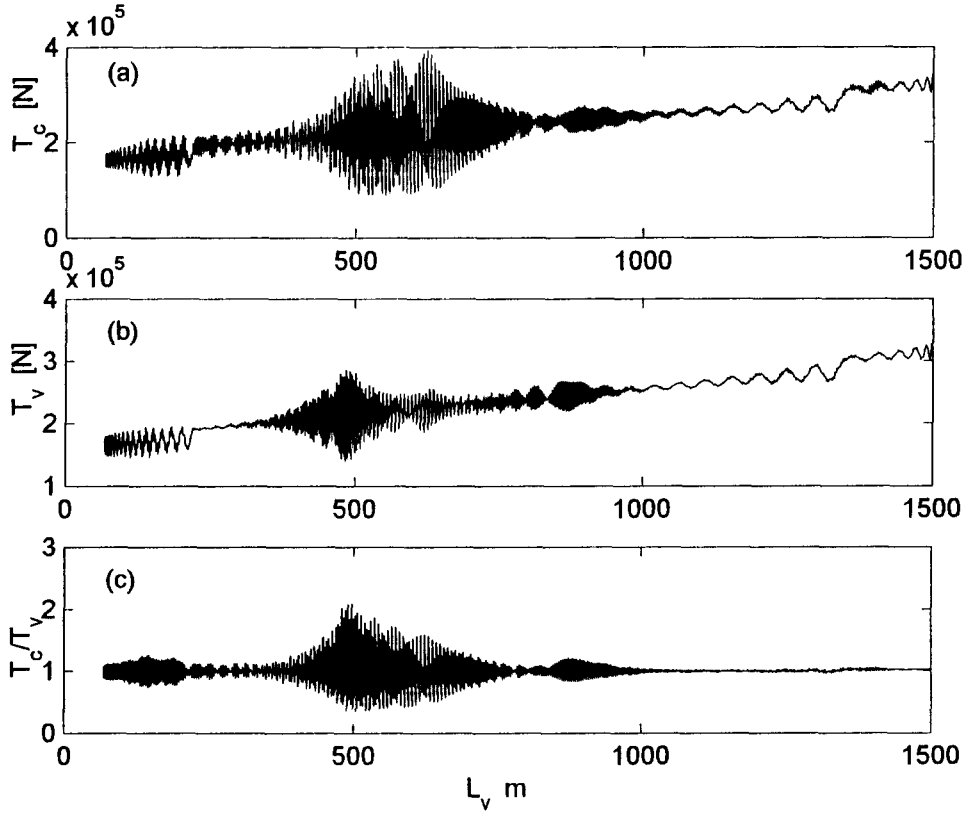

FIG. 3. *Cable Tension: (a) in catenary, (b) in vertical rope at headsheave, (c) tension ratio ocross sheave.*

discrete model equations (10)-(12). In the catenary (lateral) system a quadratic coupling between the lateral and the longitudinal modes exists, and a cubic coupling arises between the in- and out-of-plane lateral modes. In the vertical rope (longitudinal) system a quadratic coupling with the lateral modes results. The lateral system equations contain parametric excitation terms. Terms representing the inertial load due to the axial transport motion, and the cross-over external excitation are present in both systems. The natural frequencies $\bar{\omega}_n(l)$ and $\omega_n(l)$ change with time, and a passage through the primary, parametric, and autoparametric resonances may occur during the wind.

The model example simulation results show that the nonlinear coupling in the system promotes significant modal interactions during the passage through the instability region. High amplitude vibration which induces large oscillations in the cable tension is predicted. Therefore, an appropriate design methodology, as well as careful winding strategy, are required to ensure that the regions of excessive nonlinear interactions are avoided during the normal operating regimes.

ACKNOWLEDGMENT

The author gratefully acknowledges the support received from the University of Natal Research Fund.

References

[1] G. N. Savin and O. A. Goroshko 1971 *Introduction to Mechanics of One-Dimensional Bodies with Variable Length.* Kiev: Naukova Dumka (in Russian).

[2] T. Kotera 1978 *Bulletin of the JSME* 21, 1469-1474. Vibrations of String with Time-Varying Length.

[3] R. R. Mankowski 1982 *PhD Thesis, Department of Mechanical Engineering, University of the Witwatersrand, South Africa.* A Study of Nonlinear Vibrations Occurring in Mine Hoisting Cables.

[4] C. P. Constancon 1993 *PhD Thesis, Department of Mechanical Engineering, University of the Witwatersrand, South Africa.* The Dynamics of Mine Hoist Catenaries.

[5] A. Kumaniecka and J. Niziol 1994 *Journal of Sound and Vibration*, 178, 211-226. Dynamic Stability of a Rope with Slow Variability of the Parameters.

[6] R. R. Mankowski 1988 *Journal of the South African Institute of Mining and Metallurgy* 88, 401-410. Internal Damping Characteristics of a Mine Hoist Cable Undergoing Non-Planar Transverse Vibration.

[7] N. C. Perkins and C. D. Mote, Jr. 1987 *Journal of Sound and Vibration* 114, 325-340. Three-Dimensional Vibration of Travelling Elastic Cable.